

Wenhai Hu, Song Cheng, Hongying Xia*, Libo Zhang*, Xin Jiang, Qi Zhang and Quan Chen

Waste phenolic resin derived activated carbon by microwave-assisted KOH activation and application to dye wastewater treatment

<https://doi.org/10.1515/gps-2019-0008>

Received August 23, 2018; accepted October 03, 2018.

Abstract: The waste phenolic resin was utilized as the raw material to prepare activated carbon (AC) used KOH as the activating agent via microwave heating. The phenolic resin was carbonized at 500°C and then performed with a KOH/Char ratio of 4 and microwave power of 700 W for a duration of 15 min. The physic-chemical characteristics of the AC were characterized by N₂ adsorption instrument, FTIR, SEM and TEM. The BET surface area and pore volume of AC were found to be 4269 m²/g and 2.396 ml/g, respectively. The activation process to generate such a phenomenally high surface area of the AC has little reported in open literatures and could pave way for preparation adsorbents that are far superior to the currently marketed adsorbents. The methylene blue (MB) was used as the

model to assess its suitability to dye wastewater treatment. Towards this, the MB adsorption isotherms were conducted at three different temperatures and tested with different adsorption isotherm models. The adsorption isotherms could be modeled using Langmuir isotherm. While the kinetics could be used the pseudo-second order kinetics to describe. Thermodynamic results demonstrated that the adsorption process was a spontaneous, as well as an endothermic.

Keywords: activated carbon; microwave heating; wastewater treatment; adsorption

List of abbreviations

AC	Activated carbon
FTIR	Fourier Transform infrared spectroscopy
SEM	Scanning electron microscope
TEM	Transmission electron microscope
MB	Methylene blue
COD	Chemical Oxygen Demand
BOD	Biochemical Oxygen Demand

* **Corresponding authors: Hongying Xia and Libo Zhang**, State Key Laboratory of Complex Nonferrous Metal Resources Clean Utilization, Kunming University of Science and Technology, Kunming, Yunnan 650093, China; Yunnan Provincial Key Laboratory of Intensification Metallurgy, Kunming University of Science and Technology, Kunming, Yunnan 650093, China; National Local Joint Laboratory of Engineering Application of Microwave Energy and Equipment Technology, Kunming, Yunnan 650093, China, e-mail: hyxia@kmust.edu.cn, zhanglibopaper@126.com, +86 0871-65138997

Wenhai Hu, Xin Jiang, Qi Zhang and Quan Chen, State Key Laboratory of Complex Nonferrous Metal Resources Clean Utilization, Kunming University of Science and Technology, Kunming, Yunnan 650093, China; Yunnan Provincial Key Laboratory of Intensification Metallurgy, Kunming University of Science and Technology, Kunming, Yunnan 650093, China; National Local Joint Laboratory of Engineering Application of Microwave Energy and Equipment Technology, Kunming, Yunnan 650093, China

Song Cheng, State Key Laboratory of Complex Nonferrous Metal Resources Clean Utilization, Kunming University of Science and Technology, Kunming, Yunnan 650093, China; Yunnan Provincial Key Laboratory of Intensification Metallurgy, Kunming University of Science and Technology, Kunming, Yunnan 650093, China; National Local Joint Laboratory of Engineering Application of Microwave Energy and Equipment Technology, Kunming, Yunnan 650093, China; Department of Chemical Engineering, Khalifa University of Science and Technology, Abu Dhabi, United Arab Emirates

1 Introduction

Organic pollutants have received significant attention from the scientific community in the in recent years owe to the harmful impacts on human health and ecological environment [1]. Organic wastewater is produced from lots of industrial which include cottonocracy, plastics, and pulp manufacture [2]. The organic dyes in the wastewater can lead to considerable negative impacts on the environment which includes reducing light transmittance, cancerogenic substance and mutations in genes, as well as increase in the COD and BOD content of wastewater [3]. Hence it is imperative to treat the wastewater before being discharged into natural environment to reduce the impact on the natural environment. The dyes are harder to be biodegraded owing to their complex aromatic molecular structures as compared to other contaminant. And its removal utilizing conventional biological wastewater systems has been a

challenge. Hence it is imperative to develop treatment systems that could effectively treat dyes economically.

The conventional techniques include coagulation [4], hyperfiltration [5], chemical oxidation [6], filter binding assay [7], biosorption [8], and ozonation [9]. However, these approaches lack the expected degree of effectiveness technologically as well as economically. Adsorption technology has attracted our attention because of its advantages among these methods. For instance, it has higher efficiency, lower cost, and relatively easy-to-adopt [10]. AC has abundant pore structure and powerful adsorption affinity, widely being used in dyes wastewater treatment [11]. The spent phenolic resin is obtained from industrial productions. Because of its low cost and higher carbon content, phenolic resin would be used as a potential raw material to prepare the phenolic resin-based carbon materials [12].

In general, AC can be prepared either using physical or chemical activation methods. Physical activation method requires the activation gas such as steam, CO_2 , or their compound. However, the process needs a high activation temperature for a long time, leading to low production yield and high costs [13]. Chemical activation method has been widely employed in improving AC performance such as pore volume and specific surface area. And the activation agents usually include H_2SO_4 , HCl , KOH , NaOH , ZnCl_2 , K_2CO_3 , Na_2CO_3 and H_3PO_4 [14-17]. As one of the activation agents, KOH can make AC with abundant pore parameter [18-20]. Chemical activation has many advantages, which include lower activation temperatures, lower time, more abundant pore structure and higher production over physical activation [21].

Recently, microwave heating is a green heat method which has been widely applied for preparing of AC [14,15]. The transfer of heat is not by either conduction or convection, from exterior to interior having a temperature gradient from exterior to interior being nonuniform [22]. The heating utilizing of the microwave energy is uniform as the material converting the absorbed microwave energy and heats up from within itself. The main advantage of the microwave heating are lower heating time, higher heating rate and the non-contact heating way [22,23]. Therefore, microwave heating is applied in various manufacturing industries and considered to be a mature and promising processing technology. The present work utilizes the advantages of the microwave heating for conversion of waste phenolic resin into AC with KOH as the activating agent. The prepared AC is characterized by nitrogen adsorption isotherms, FTIR, SEM and TEM. And then the prepared AC would be used to treat the wastewater to study its adsorption performance.

2 Experimental material and method

2.1 Material

The raw material is collected from a company in China. The KOH and MB are both chemical reagent that purchased from China.

2.2 Experimental methods

Firstly, the raw material was heated via conventional coking furnace at the temperature of 500°C for 2 h under inert gas to obtain the char. 8 g char and 32 g KOH were mixed with the mass ratio of 1:4. And then the impregnated mixture was putted into microwave oven with microwave power of 700 W for 15 min. After cooling, AC was washed by HCl solution and then washed by distilled water. Finally, it filtered and dried, and stored in dry environment for characterization.

2.3 Characterization of AC

The pore structural parameters of the AC were tested by the nitrogen adsorption instrument (Autosorb-1-C, USA) at 77 K. Scanning electron microscope (SEM, Philips XL30ESEM-TMP) and transmission electron microscope (TEM, JEM-2100, Japan) was used to analyze the surface structure of the AC. The surface functional groups of AC and char were used FTIR (Thermo Nicolet Co., USA) to observe.

2.4 Adsorption isotherms

The adsorption performance of the AC was evaluated by the MB. Series of the adsorption experiments were did in the conical flasks. 0.1 g AC was mixed with the 100 ml MB solution with concentration of 200-400 mg/L, and then put into the gas bath thermostatic at the temperature of $30-50^\circ\text{C}$ with the speed of 300 r/min until the equilibrium. The residual MB amount was calculated by UV-vis spectrophotometer. And then the absorbed amount of MB on AC, q_e (mg/g), was calculated using the following expression:

$$q_e = (C_0 - C_e) V / M \quad (1)$$

where C_0 (mg/L) is the initial concentrations of MB solutions, and C_e (mg/L) is the equilibrium concentrations of MB solutions. V and M are the volume of solution (L) and the weight of the adsorbent (g), respectively.

2.5 Adsorption kinetics

The kinetics experiments were also did in the conical flasks. And it was similar with the adsorption isotherms experiment. The mixed solution was sampled at regular time. The MB concentration adsorbed per time could be calculated via the following equation:

$$q_t = (C_0 - C_t)V/M \quad (2)$$

where C_t is MB liquid-phase concentration.

3 Result and discussion

3.1 Pore structure analysis

Figure 1 shows the N₂ adsorption isotherms of AC and char [24]. This kind of adsorption isotherms is belonged to a type I isotherms on the basis of IUPAC classification. As Figure 1 shown, it manifests that absorption volume of AC is much greater than that char, demonstrating tremendous increase in the pore volume of the AC. The pore size distribution of AC and char is shown in Figure 2. As seen in Figure 2, the pore volume of the AC is obviously large in the micropore region, evidencing the reaction of KOH-C producing large quantities of micropores.

Table 1 shows the pore parameter of the AC and char [24]. Compared with the char, the total pore volume and the surface area tremendously increase for AC. Such high surface area has little reported in open literatures, which could possibly be attributed to the effectiveness of KOH activation in a microwave heating mode.

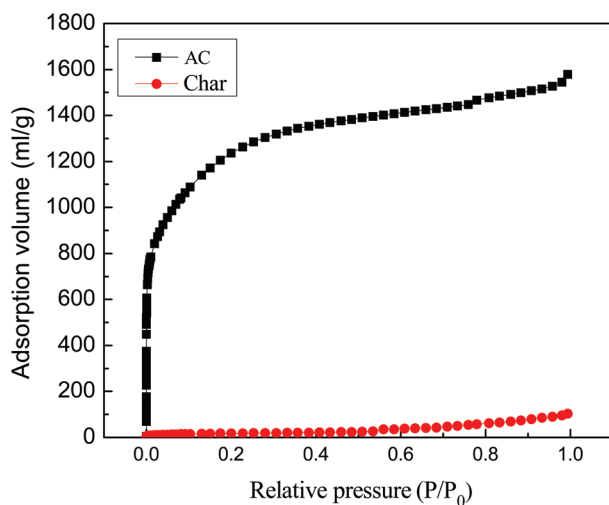


Figure 1: Nitrogen adsorption isotherm pore size distribution of the AC and char.

3.2 FTIR analysis of AC and char

Figure 3 shows FTIR spectra of AC and char. It can be observed that there is little different from AC and char, based on Figure 3. The spectrum of the AC has peaks at 3435, 2925, 1630 and 1120 cm⁻¹. While the spectrum of the char has peaks at 3443, 2914, 1697, 875 and 750 cm⁻¹. The wavebands in the region of 3440–3420 cm⁻¹ are attributed

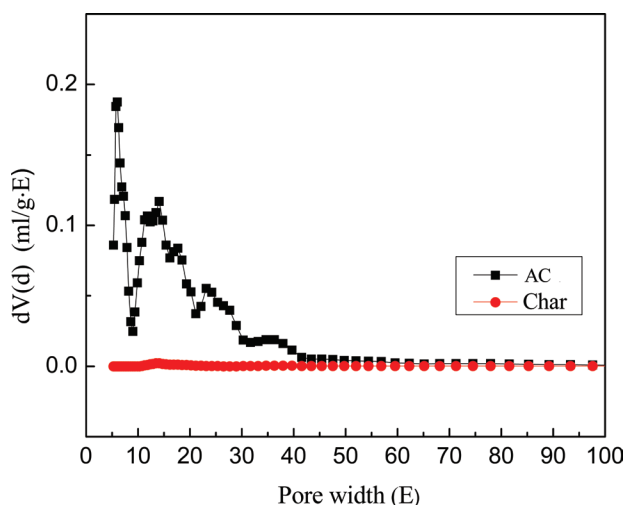


Figure 2: Pore size distribution (c) of the AC and char.

Table 1: Pore structural parameters of the char and AC.

	S_{BET} (m ² /g)	V_{tot} (ml/g)	D_a (Å)	V_{mic} (ml/g)	S_{mic} (m ² /g)	S_{external} (m ² /g)	V_{mes} (ml/g)	$V_{\text{mic}}/V_{\text{tot}}$ (%)
Char	33	0.041	50.0	0.001	3	30	0.040	2.46
AC	4269	2.396	22.5	1.690	3561	708	0.706	70.53

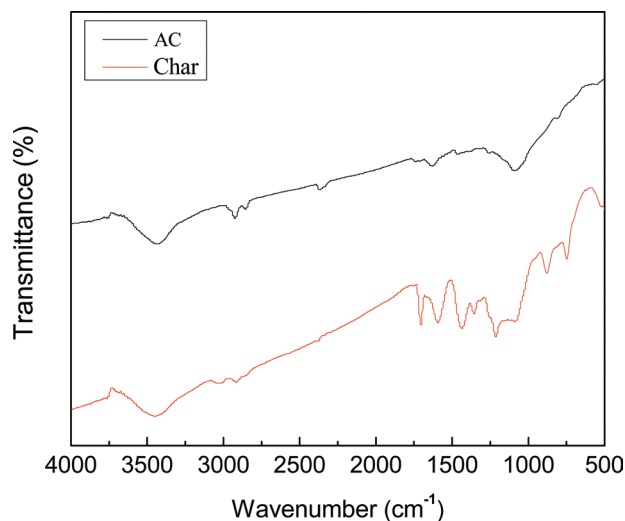


Figure 3: Fourier transform infrared spectroscopy (FTIR) spectra of the AC and char.

to O-H stretching vibration [25]. The intense band at about 2925 cm^{-1} and its shoulder at 2914 cm^{-1} are attributed to C-H stretching vibration [26]. The peak at the 1697 cm^{-1} indicates C-C symmetrical stretching of pyrone, while the low peak at 1630 cm^{-1} is attributed to vibration of H-O-H from absorbed water [27,28]. Strong peaks at 875 cm^{-1} belongs to poly substituted aromatic ring, while the one at 750 cm^{-1} corresponds to 1, 2 C=C stretching in the aromatic rings, respectively [16,22]. Finally, the peak at 1120 cm^{-1} is phenol C-O stretching [29]. Compared the FTIR spectrum of char with AC, the bands of char ranging from 1679 to 1120 cm^{-1} disappears.

3.3 Adsorption isotherms

Adsorption isotherms are employed to study adsorption process, which helps to understand how the molecules are adsorbed onto the surface of AC. Four different popular

adsorption isotherm models are used to analyze experiment data to choose the best model. The models attempted in this work are compiled in Table 2, which provides the details of the model equations. Table 3 lists the calculated fitting parameters of these models. The correlation coefficient (R^2) of the Langmuir isotherm is the largest based on the Table 3. The adsorption amount of the MB is increase with the temperature increasing. The monolayer adsorption capacity was in the range of 460.8 to 485.4 mg/g which is far higher than the adsorption capacity of most adsorbents that has been reported in literatures.

Table 4 summarizes the comparison of the MB adsorption capacity, BET and the $V_{\text{mic}}/V_{\text{tot}}$ of various of AC. The MB adsorption capacity in this study is larger than those reported [30-33], suggesting that the AC have great potential application in MB removal. As shown in Table 4, the BET of the AC that prepared from phenolic resin (phenolic resin-AC) is the biggest than other kinds of AC. But, the adsorption capability of the

Table 2: Adsorption isotherm models adopted in this work and their parameters.

Isotherm	Equation	Parameters
Langmuir	$\frac{1}{q_e} = \frac{1}{k_L Q_0 C_e} + \frac{1}{Q_0}$	C_e is the equilibrium concentration (mg/L) Q_0 (mg/g) is adsorption constant related to adsorption capacity k_L (L/g) is adsorption constant related to energy of adsorption
Freundlich	$\ln(q_e) = \ln(k_F) + \frac{1}{n} \ln(C_e)$	k_F is adsorption constant related to adsorption capacity (mg/g).(L/mg) $^{1/n}$ n is adsorption constant measuring the adsorption intensity
Dubinin-Radushkevich	$\ln q_e = \ln \alpha - \beta R^2 T^2 \left[\ln \left(1 + \frac{1}{C_e} \right) \right]^2$	α is the adsorption capacity (mg g $^{-1}$) β is the constant related to the adsorption energy (mol 2 kj $^{-2}$)
Temkin	$q_e = A + B \ln(C_e)$	A and B are constants

Table 3: Adsorption isotherm parameters at different temperatures.

Isotherms	Parameters	Temperature (K)		
		303	313	323
Langmuir	Q_0 (mg/g)	460.8	473.9	485.4
	K_L (L/mg)	1.1667	1.2712	1.5489
	R^2	0.99	0.99	0.99
Freundlich	$1/n$	2.6785	2.6106	2.8255
	K_F (mg/g).(L/mg) $^{1/n}$	240.36	255.13	281.14
	R^2	0.99	0.98	0.94
Dubinin-Radushkevich	α (mg g $^{-1}$)	374.95	384.58	397.64
	β (mol 2 j $^{-2}$) 10^{-8}	11.96	9.96	7.37
	E (KJ/mol)	2.04	2.24	2.60
Temkin	R^2	0.90	0.94	0.98
	R^2	0.99	0.98	0.98

Table 4: The MB adsorption capability of the different kinds AC.

Adsorbents	BET	$V_{\text{mic}}/V_{\text{tot}}$ (%)	Adsorption capacity (mg/g)	References
AC	4269	70%	485.4	This study
Biodiesel industry solid residue-AC	1372	42.11%	395.3	[30]
Regeneration	621.51	47.45%	410.85	[31]
Durian shell-AC	1233	64.63%	375.93	[32]
Spent coal-AC	1100	70%	277	[33]
Cashew nut-AC	1478	37%	352	[33]
−0.5				
Cashew nut-AC	859	22%	263	[33]
−1.5				
Cashew nut-AC −2	875	58%	215	[33]
Cashew nut-AC −1				

MB is only 20% more large than that AC prepared from biodiesel industry solid residue (The BET of the phenolic resin-AC is three times more than that the AC prepared from biodiesel industry solid residue). The reason may be that the micropore volume of the phenolic resin-AC has the 70% of the total volume indicating having lots of the micropore. The pore size of these micropore isn't big enough to adsorb the MB molecule. So, the MB adsorption capability of the AC is only 20% more large than that AC prepared from biodiesel industry solid residue. Kasaoka et al. reported that adsorption occurred when the pore diameter of adsorbent at least 1.7 times as much as of the adsorbate [34]. The minimum molecular size of MB is about 0.8 nm, while the average pore sizes of phenolic resin-AC is 2.25 nm. Therefore, it is accessible adsorption MB molecule. If the pore size is not big enough, it cannot adsorb the big MB molecule. As shown in Table 4, the BET of the cashew nut-AC-1 is larger than that cashew nut-AC-2. But the MB adsorption capability of the cashew nut-AC-1 is lower than that cashew nut-AC-2. The reason is that the cashew nut-AC-1 has the bigger V_{mic}/V_{tot} . But if the BET is bigger enough, we can neglect the impact of the V_{mic}/V_{tot} on MB adsorption capability. (See the different between cashew nut-AC -0.5 and cashew nut-AC -1). Although the cashew nut-AC -0.5 has the bigger V_{mic}/V_{tot} , it also has the larger MB adsorption capability.

Langmuir isotherm most suitably represents the adsorption data. Another characteristic parameter that can be used to evaluate adsorbents on Langmuir isotherm is dimensionless factor R_L , which is calculated by:

$$R_L = \frac{1}{1 + K_L C_0} \quad (3)$$

In the above formula C_0 is MB initial concentration and K_L is Langmuir constant. The value of R_L is depends on the type of isotherm: unfavorable ($R_L > 1$), linear ($R_L = 1$), favorable ($0 < R_L < 1$), irreversible ($R_L = 0$). The calculation R_L value is 0.1717-0.5831, demonstrating the favorable of the MB adsorption onto AC. Langmuir isotherms are shown in Figure 4 at 30-50°C.

In addition, the adsorption process was also analyzed using Dubinin-Radushkevich model. The E ($1/\sqrt{2\beta}$) was defined as the change in the free energy of an adsorbate in it solution moving from infinity to the surface of solid. The E is applied to estimate adsorption process whether it is physical or chemical adsorption. The E is found to be in the range from 2.04 to 2.6 kJ/mol, which indicates that the adsorption process could be predominately by physical adsorption, based on $E < 8$ kJ/mol.

3.4 Adsorption kinetics

Adsorption kinetics plays a formidable role in the design and sizing of the separation process equipment. Kinetics models such as Pseudo-first order, pseudo-second order, intraparticle diffusion and Elovich are employed to test experiment result so as to choose the most suitable model. Table 5 lists related model parameters. The fitting parameters of these models show in Table 6. The experimental result is agreement in pseudo-second-order model and R^2 approaches to 1. Compared with the experimental data ($q_{e,exp}$), Table 6 also provides the calculation $q_{e,cal}$ using the

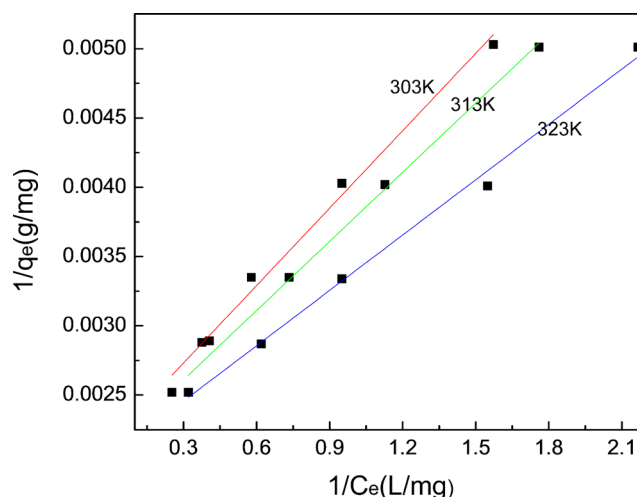


Figure 4: Langmuir isotherms for methylene blue adsorption onto AC at different temperatures.

Table 5: Adsorption Kinetic models adopted in this work and their parameters.

Kinetic models	Equation	Parameters
Pseudo-first order	$\ln(q_e - q_t) = \ln q_e - k_1 t$	q_e is the uptake of methylene blue at equilibrium (mg/g). K_1 (1/min) is the adsorption rate constant,
Pseudo-second order	$\frac{t}{q_t} = \frac{1}{K_2 q_e^2} + \frac{t}{q_e}$	K_2 (g/mg min) is the rate constant of second-order equation
Intraparticle diffusion	$q_t = K_3 \sqrt{t} + C$	K_3 (mg/g min ^{1/2}) is the intraparticle diffusion rate constant C is a constant
Elovich	$q_e = \frac{1}{b} \ln ab + \frac{1}{b} \ln t$	a (mg/g min) is the initial adsorption rat b (g/mg) is related to the extent of surface coverage and activation energy.

pseudo-second-order model ($q_{e,cal}$), manifesting that there are very consistent. This finding is also consistent with previous studies on the adsorption of MB on the biodiesel industry solid residue [35] and Siris seed pods [21] based-AC. Figure 5 presents Pseudo-second-order model of the MB adsorption at different initial concentration.

3.5 Adsorption thermodynamics

The following equations are used to estimate the thermodynamic parameters of the ΔS , ΔH and ΔG :

$$\ln K_d = \frac{\Delta S}{R} - \frac{\Delta H}{RT} \tag{4}$$

$$\Delta G = -RT \ln(K_d) \tag{5}$$

$$K_d = \frac{q_e W}{C_e V} \tag{6}$$

Table 6: Adsorption kinetics parameters at 30°C.

C_0 (mg/L)	Pseudo-first-order model			
	qe.exp (mg/L)	qe.cal (mg/L)	K_1 (1/min)	R^2
200	198.95	1.98	0.009	0.97
250	248.71	3.55	0.016	0.92
300	298.66	5.33	0.015	0.89
350	348.133	4.47	0.011	0.91
400	397.45	7.55	0.012	0.88

C_0 (mg/L)	Pseudo-second-order model			
	qe.exp (mg/L)	qe.cal (mg/L)	K_2 (g/mg min)	R^2
200	198.95	188.68	0.018	1
250	248.71	248.76	0.011	1
300	298.66	299.40	0.007	0.99
350	348.13	348.43	0.008	0.99
400	397.45	398.41	0.004	0.99

C_0 (mg/L)	Intraparticle diffusion model			
	qe.exp (mg/L)	C (mg/g)	K_3 (mg/gmin ^{1/2})	R^2
200	198.95	196.73	0.139	0.96
250	248.71	245.99	0.183	0.96
300	298.66	294.35	0.291	0.95
350	348.133	343.31	0.317	0.85
400	397.45	387.65	0.686	0.79

C_0 (mg/L)	Elovich kinetic models			
	qe.exp (mg/L)	1/blnab (mg/g)	1/b (mg/g)	R^2
200	198.95	195.19	0.650	0.96
250	248.71	249.01	0.849	0.94
300	298.66	291.09	1.368	0.97
350	348.133	339.59	1.528	0.92
400	397.45	379.25	3.385	0.89

With regard to MB, parameters such as ΔH and ΔS could be got via the slope and intercept of the Van't Hoff graph of $\ln K_d$ and $1/t$ (Figure 6). The ΔG could be obtained by Eq. 5. Table 7 shows the activation energy and adsorption thermodynamics. The values of ΔG (-12.97, -14.03, -15.17 KJ/mol) is negative at 30-50°C, which manifest that adsorption process is spontaneous and feasible [25]. The

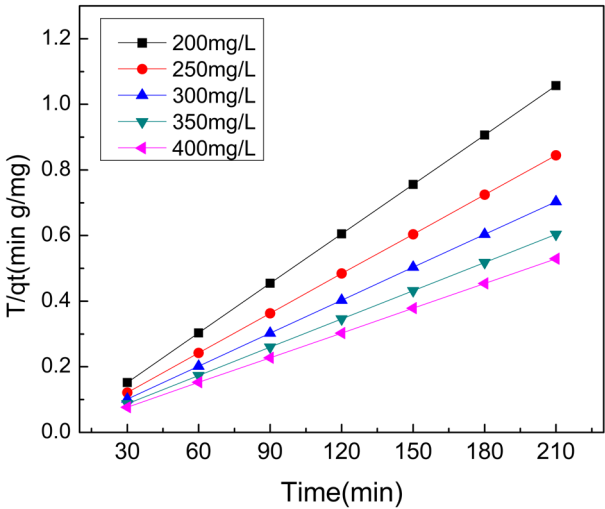


Figure 5: Pseudo-first-order kinetics for adsorption of methylene blue onto AC at 298 K.

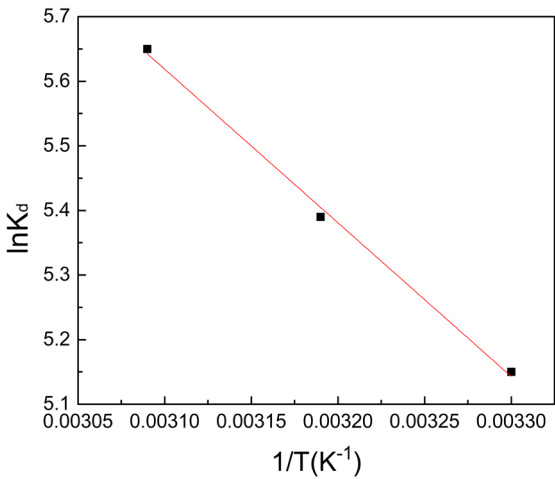


Figure 6: Van't Hoff plot $\ln K_d$ versus $1/T$ for methylene blue adsorption on HSAAC.

Table 7: Activation energy and thermodynamic parameters.

ΔH (KJ/mol)	ΔS (J/mol)	ΔG (KJ/mol)		
		303 K	313 K	323 K
19.77	107.99	-12.97	-14.03	-15.17

results were similar the Moniruzzaman et al. [18]. As the temperature increases, the negative value of G decreases, indicating that MB adsorption process is easier as temperature increasing. The positive values of ΔH (19.77 kJ/mol) indicates that the adsorption process has confirmed the physical adsorption. The adsorption reaction is the heat absorption property of AC based on the adsorption of MB with ΔH less than 80 kJ/mol. At the same time, positive ΔS (107.99 J/mol) indicates that the affinity of AC to MB and randomness of solid interface increase [26].

4 Conclusion

The waste phenolic resin is a kind of solid waste, which could be used to prepare the AC by microwave heat and KOH as agent. The prepared AC is found to possess BET surface area of 4269 m²/g, average pore diameter 2.25 nm and pore volume of 2.396 cm³/g. The utility of the AC for dye wastewater applications is tested by the organic dye model of the MB, which had a monolayer adsorption capacity in the range of 460.8 to 485.4 mg/g far higher than the popular adsorbents commonly reported in literature. The adsorption isotherms were found to match with Langmuir isotherm model while the adsorption kinetics could be modelled using a pseudo-second-order kinetic model. The adsorption is endothermic and spontaneously in nature based on thermodynamic result.

Acknowledgements: The authors would like to express their gratitude to the Specialized Research Fund for the National Natural Science Foundation of China (21567013).

References

- [1] Ahmed M.J., Theydan S.K., Microporous activated carbon from Siris seed pods by microwave-induced KOH activation for metronidazole adsorption. *J. Anal. Appl. Pyrol.*, 2013, 99, 101-109.
- [2] Alventosa D., Barredo D., Alcaina M., Iborra C., Ultrafiltration technology with a ceramic membrane for reactive dye removal: optimization of membrane performance. *J. Hazard. Mater.*, 2012, 209-210, 492-500.
- [3] Anirudhan T.S., Radhakrishnan P.G., Thermodynamics and kinetics of adsorption of Cu(II) from aqueous solutions onto a new cation exchanger derived from tamarind fruit shell. *J. Chem. Thermodyn.*, 2008, 40, 702-709.
- [4] Auta M., Hameed B.H., Chitosan-clay composite as highly effective and low-cost adsorbent for batch and fixed-bed adsorption of methylene blue. *Chem. Eng. J.*, 2014, 237, 352-361.
- [5] Auta M., Hameed B.H., Preparation of waste tea activated carbon using potassium acetate as an activating agent for adsorption of Acid Blue 25 dye. *Chem. Eng. J.*, 2011, 171, 502-509.
- [6] Bai Y., Huang Z.H., Kang F., Electrospun preparation of microporous carbon ultrafine fibers with tuned diameter, pore structure and hydrophobicity from phenolic resin. *Carbon*, 2014, 66, 705-712.
- [7] Cheng S., Zhang L., Xia H., Peng J., Shu J., Ultrasound and microwave-assisted preparation of Fe-activated carbon as an effective low-cost adsorbent for dyes wastewater treatment. *RSC Adv.*, 6/82, 2016.
- [8] Cheng S., Zhang, L., Xia, H., Peng, J., Shu, J., Zhang Q., et al., Adsorption behavior of methylene blue onto waste-derived adsorbent and exhaust gases recycling. *RSC Adv.*, 2017, 7, 27331-27341.
- [9] Foo K.Y., Hameed B.H., Preparation and characterization of activated carbon from pistachio nut shells via microwave-induced chemical activation. *Biomass Bioenerg.*, 2011, 35, 3257-3261.
- [10] Foo K.Y., Hameed B.H., Microwave-assisted preparation and adsorption performance of activated carbon from biodiesel industry solid residue: Influence of operational parameters. *Bioresour. Technol.*, 2012, 103, 398-404.
- [11] Ghaedi M., Hajati S., Barazesh B., Karimi F., Ghezlbash G., Equilibrium, kinetic and isotherm of some metal ion biosorption. *J. Ind. Eng. Chem.*, 2013, 19, 227-233.
- [12] Gregg S.J., Ramsay J.D., Adsorption of carbon dioxide by magnesia studied by use of infrared and isotherm measurements. *J. Chem. Soc. A Inorg. Phys. Theor.*, 1970, 2784-2787.
- [13] Huang, Y., Ma E., Zhao G., Thermal and structure analysis on reaction mechanisms during the preparation of activated carbon fibers by KOH activation from liquefied wood-based fibers. *Ind. Crop. Prod.*, 2015, 69, 447-455.
- [14] Hui D., Li G., Yang H., Tang J., Tang J., Preparation of activated carbons from cotton stalk by microwave assisted KOH and K₂CO₃ activation. *Chem. Eng. J.*, 2010, 163, 373-381.
- [15] Ji Y., Li T., Li Z., Wang X., Lin Q., Preparation of activated carbons by microwave heating KOH activation. *App. Surf. Sci.*, 2007, 254, 506-512.
- [16] Kubota M., Hata A., Matsuda H., Preparation of activated carbon from phenolic resin by KOH chemical activation under microwave heating. *Carbon*, 2009, 47, 2805-2811.
- [17] Mishra S., Mukul A., Sen G., Jha U., Microwave assisted synthesis of polyacrylamide grafted starch (St-g-PAM) and its applicability as flocculant for water treatment. *Int. J. Biol. Macromol.*, 2011, 48, 106-111.
- [18] Moniruzzaman M., Ono T., Separation and characterization of cellulose fibers from cypress wood treated with ionic liquid prior to laccase treatment. *Bioresour. Technol.*, 2013, 127, 132.

- [19] Muniandy L., Adam F., Mohamed A.R., Ng E.P., The synthesis and characterization of high purity mixed microporous/mesoporous activated carbon from rice husk using chemical activation with NaOH and KOH. *Micropor. Mesopor. Mater.*, 2014, 197, 316-323.
- [20] Nabais J.M.V., Carrott P.J.M., Carrott M.M.L.R., Menéndez J.A., Preparation and modification of activated carbon fibres by microwave heating. *Carbon*, 2004, 42, 1315-1320.
- [21] Shuang-Chen MA., Mao X.Y., Guo T.X., Zhao Y., Experimental study on desulfurization and denitrification from flue gas over modified activated carbon using microwave irradiation. *J. Fuel Chem. Technol.*, 2010, 38, 739-744.
- [22] Tünay O., Kabdaslı I., Eremektar G., Orhon D., Color removal from textile wastewaters. *Water Sci. Technol.*, 1996, 34, 9-16.
- [23] Tehranibagha A.R., Mahmoodi N.M., Menger F.M., Degradation of a persistent organic dye from colored textile wastewater by ozonation. *Desalination*, 2010, 260, 34-38.
- [24] Cheng S., Zhang L.B., Zhang S.Z., Xia H.Y., Peng J.H., Preparation of high surface area activated carbon from spent phenolic resin by microwave heating and KOH activation. *High Temp. Mater. Proc.*, 2018, 37, 59-68.
- [25] Wang J., Kaskel S., KOH activation of carbon-based materials for energy storage. *J. Mater. Chem.*, 2012, 22, 23710-23725.
- [26] Yang J.B., Ling L.C., Liu L., Kang F.Y., Huang Z.H., Wu H., Preparation and properties of phenolic resin-based activated carbon spheres with controlled pore size distribution. *Carbon*, 2002, 40, 911-916.
- [27] Ji Y., Li T., Li Z., Wang X., Lin Q. Preparation of activated carbons by microwave heating KOH activation. *Appl. Surf. Sci.*, 2007, 254, 506-512.
- [28] Moniruzzaman M., Ono T., Separation and characterization of cellulose fibers from cypress wood treated with ionic liquid prior to laccase treatment. *Bioresource Technol.*, 2013, 127, 132-137.
- [29] Zhao Y., Yan N., Feng M.W., Thermal degradation characteristics of phenol-formaldehyde resins derived from beetle infested pine barks. *Thermochim. Acta*, 2013, 555, 46-52.
- [30] Foo K.Y., Hameed B.H., Microwave-assisted preparation and adsorption performance of activated carbon from biodiesel industry solid residue: Influence of operational parameters. *Bioresource Technol.*, 2012, 103, 398-404.
- [31] Foo K.Y., Hameed B.H., A cost effective method for regeneration of durian shell and jackfruit peel activated carbons by microwave irradiation. *Chem. Eng. J.*, 2012, 193-194.
- [32] Duan X.H., Srinivasakannan C., Liang J.S., Process optimization of thermal regeneration of spent coal based activated carbon using steam and application to methylene blue dye adsorption. *J. Taiwan Inst. Chem. E.*, 2014, 45, 1618-1627.
- [33] Spagnoli A.A., Dimitrios A.G., Svetlana B., Adsorption of methylene blue on cashew nut shell based carbons activated with zinc chloride: The role of surface and structural parameters. *J. Mol. Liq.*, 2017, 229, 465-229, 471.
- [34] Kasaoka S., Sakata Y., Tanaka E.R., Design of molecular sieving carbon-studies on adsorption of various dyes in liquid phase. *Int. Chem. Eng.* 1989, 29, 734-742.
- [35] Gang X., Rongbing W., Huilong Z., Mingjiang N., Xiang G., Kefa C., Preparation and characterization of activated carbons based alkali lignin by KOH chemical activation. *J. Combustion Sci. Technol.*, 2014, 20, 14-20.